GEOPHYSICAL RESEARCH LETTERS, VOL. 41, 96–101, doi:10.1002/2013GL058048, 2014

Seabed fluid expulsion along the upper slope and outer shelf of the U.S. Atlantic continental margin

D. S. Brothers,[1] C. Ruppel,[1] J. W. Kluesner,[2] U. S. ten Brink,[1] J. D. Chaytor,[1] J. C. Hill,[3] B. D. Andrews,[1] and C. Flores[1]

Received 17 September 2013; revised 3 December 2013; accepted 5 December 2013; published 8 January 2014.

[1] Identifying the spatial distribution of seabed fluid expulsion features is crucial for understanding the substrate plumbing system of any continental margin. A 1100 km stretch of the U.S. Atlantic margin contains more than 5000 pockmarks at water depths of 120 m (shelf edge) to 700 m (upper slope), mostly updip of the contemporary gas hydrate stability zone (GHSZ). Advanced attribute analyses of high-resolution multichannel seismic reflection data reveal gas-charged sediment and probable fluid chimneys beneath pockmark fields. A series of enhanced reflectors, inferred to represent hydrate-bearing sediments, occur within the GHSZ. Differential sediment loading at the shelf edge and warming-induced gas hydrate dissociation along the upper slope are the proposed mechanisms that led to transient changes in substrate pore fluid overpressure, vertical fluid/gas migration, and pockmark formation. **Citation:** Brothers, D. S., C. Ruppel, J. W. Kluesner, U. S. ten Brink, J. D. Chaytor, J. C. Hill, B. D. Andrews, and C. Flores (2014), Seabed fluid expulsion along the upper slope and outer shelf of the U.S. Atlantic continental margin, *Geophys. Res. Lett.*, *41*, 96–101, doi:10.1002/2013GL058048.

1. Introduction

[2] As geomorphic features, pockmarks generally indicate past and/or ongoing fluid expulsion across the sediment-water interface [*Berndt*, 2005; *Judd and Hovland*, 2007]. Determining the geological significance of pockmarks along passive continental margins requires constraints on fluid sources and substrate migration pathways. Several processes drive seabed fluid expulsion, including sediment loading/compaction, gas hydrate dynamics, hydrocarbon leakage, submarine freshwater discharge, and diagenesis (see original references in *Berndt* [2005] and *Judd and Hovland* [2007]).

[3] Although published evidence for seabed fluid expulsion along the continental shelf edge and slope of the U.S. Atlantic margin (USAM) is relatively sparse [*Hill et al.*, 2004; *McHugh et al.*, 1993; *Newman et al.*, 2008], recent *Okeanos Explorer* missions discovered active gas seeps along both regions [e.g., *Skarke et al.*, 2013]. Previous studies aimed at understanding the sources of substrate overpressure and fluid migration on this margin were based largely on modeling results, yielding two primary hypotheses for potential sources of fluid expulsion: pore fluid overpressure from differential sediment compaction [*Dugan and Flemings*, 2002] and gas hydrate dissociation due to recent warming of ocean bottom water [*Hill et al.*, 2004; *Phrampus and Hornbach*, 2012]. Here we present new constraints on the spatial distribution of fluid expulsion features along the upper slope/outer shelf of the USAM and evaluate the potential fluid sources using nested high-resolution multibeam bathymetric data and meta-attribute analyses applied to multichannel seismic reflection profiles.

2. Geologic Setting

[4] The Quaternary geologic history of the USAM was shaped by glacial/interglacial cycles and extreme variations in sea level. During eustatic sea level low stands, large river and glacial drainage systems from Virginia to Maine transported siliciclastic sediments to the shelf edge [*Poag and Sevon*, 1989]. The Mid-Atlantic and New England sections of the margin are characterized by relatively narrow (<5 km), seaward thickening wedges of shelf edge delta deposits (200–400 m thick) that are heavily dissected by submarine canyons [e.g., *Brothers et al.*, 2013]. In contrast, the shelf edge and upper slope of the Hudson Apron and southern New England sections are smooth (i.e., widely spaced canyons), broad, and gently inclined. During the Pleistocene, up to 18 km of shelf edge progradation [*Mountain et al.*, 2007] produced thick sequences that can be continuously traced from the shelf edge to the uppermost rise in some places [*Brothers et al.*, 2013]. These sequences provide a rare opportunity to examine variations in stratigraphic character across regionally conformable depositional surfaces.

[5] The depositional history of the Hudson Apron continental slope was explored at Ocean Drilling Program (ODP) Site 1073 [*Austin et al.*, 1998], which was drilled to 663 m below seafloor (mbsf) at a water depth of 639 m. Correlation among seismic reflectors, lithology, and isotopic records constrains major Pleistocene sequence stratigraphic boundaries [*Austin et al.*, 1998]. Each sequence is dominated by a succession of clay- and silt-rich sedimentary facies that were correlated to oxygen isotope records [*McHugh and Olson*, 2002], with coarser-grained facies marking glacial-interglacial transitions. The underlying Pliocene and Miocene sections have higher sand content and porosity [*Austin et al.*, 1998]. The near-seafloor section contains very thin (<1 m) or nonexistent Holocene sediment that overlies

Additional supporting information may be found in the online version of this article.

[1]Woods Hole Coastal and Marine Science Center, U.S. Geological Survey, Woods Hole, Massachusetts, USA.
[2]Earth and Planetary Sciences, University of California, Santa Cruz, California, USA.
[3]Center for Marine and Wetland Studies, Coastal Carolina University, Conway, South Carolina, USA.

Corresponding author: D. S. Brothers, Woods Hole Coastal and Marine Science Center, U.S. Geological Survey, 384 Woods Hole Rd., Woods Hole, MA 02543, USA. (dbrothers@usgs.gov)

0094-8276/14/10.1002/2013GL058048

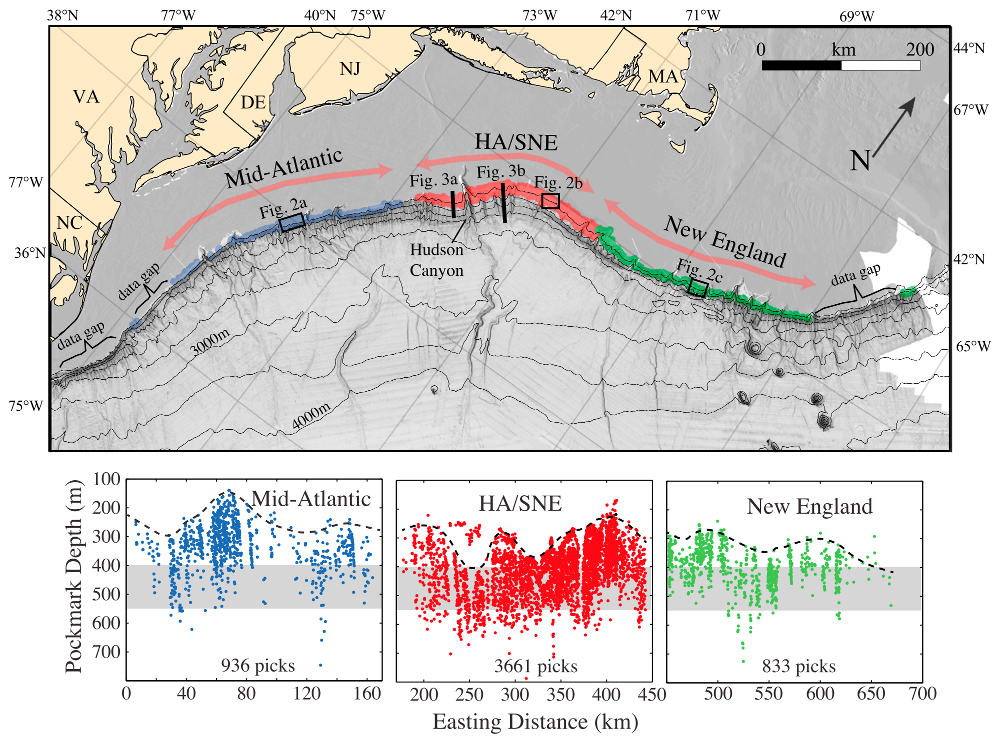

Figure 1. (top) Shaded relief bathymetry (500 m contours) of the U.S. Atlantic margin [*Andrews et al*., 2013]. Pockmarks are overlain as transparent points and colored according to geomorphic sector. Bold lines are locations of MCS profiles in Figure 3. (bottom) Pockmark distribution with water depth in the three sectors along the margin. Dashed lines represent approximate landward extend of continuous multibeam bathymetry coverage; gray shading shows permissible water depths for the upslope extent of gas hydrate stability assuming bottom water temperature between 3°C (~400 m water depth) and contemporary values (~550 m water depth). Pockmark-free zones are generally associated with either large, shelf-indenting submarine canyons or data gaps.

late Pleistocene material deposited during and after the Last Glacial Maximum (LGM) [*McHugh et al*., 2010].

3. Data and Methods

[6] NOAA ships *Okeanos Explorer* and *Nancy Foster* acquired most of the shelf and upper slope bathymetric data used in this study; other cruises provided multibeam bathymetric coverage of the slope and upper rise from North Carolina to Canada [*Andrews et al*., 2013]. With a few exceptions, the high-resolution bathymetric data extend slightly landward of the shelf edge rollover at 110–250 m below sea level (mbsl). Raw data were edited, processed, and gridded at 25 m, 50 m, and 100 m for regions shallower than 1000 mbsl, between 1000 and 2000 mbsl, and greater than 2000 mbsl, respectively. Selected regions along the shelf edge were gridded on 10 m cells. The margin was split into the Mid-Atlantic, Hudson Apron/southern New England, and New England sections based on the first-order morphology of the continental shelf, slope, and rise (Figure 1) [*Brothers et al*., 2013]. Within each section, pockmarks were mapped at a 1:75,000 scale, and their locations, water depths, and approximate dimensions (relief and diameter) were extracted using ESRI ArcGIS (Figures 1 and 2).

[7] Two high-resolution multichannel seismic (MCS) reflection profiles across the outer shelf and upper continental slope were used as representative transects: OC270 Profile-61 crosses ODP Site 1073 on the Hudson Apron, while Tiki2011 Profile-04 spans the continental slope and upper rise ~45 km east of Hudson Canyon (Figure 1 and supporting information Figure S1). The latter profile was acquired as part of a 2010 and 2011 *M/V Tiki XIV* program that obtained ~1600 km of 72-channel (6.25 m group spacing) data along the shelf edge and slope of the Hudson Apron and southern New England sections of the USAM. A 6 kJ sparker source provided peak frequencies between 90 and 300 Hz, yielding ~5 m vertical resolution and ~1 km of penetration. Migrated, common depth point stacks were band pass filtered (50–200 Hz) and integrated with reprocessed 48-channel (12.5 m group spacing), 90 in^3 GI-gun source, MCS profiles that had earlier been collected aboard the *R/V Oceanus* in 1996 (e.g., OC270 Profile-61), and the *R/V Endeavor* in 2002 (supporting information Figure S1).

[8] Post processing, MCS profiles were conditioned for advanced attribute analyses using OpendTect software. First, dip steering was used to record the local dip and azimuth of seismic horizons at every sample position, followed by dip-steered median filtering to sharpen discontinuities along seismic horizons and to enhance laterally continuous reflectors. Second, average energy and instantaneous frequency attributes, as well as gas-chimney meta-attributes, were calculated. The energy and frequency calculations measure reflectivity and peak frequency in a specified time gate (e.g., 10 ms) and are used to identify lateral variations in reflector character. The chimney meta-attribute combines several seismic parameters into a single probability attribute that can be used to quantify reflector discontinuities caused by gas chimneys and fluid

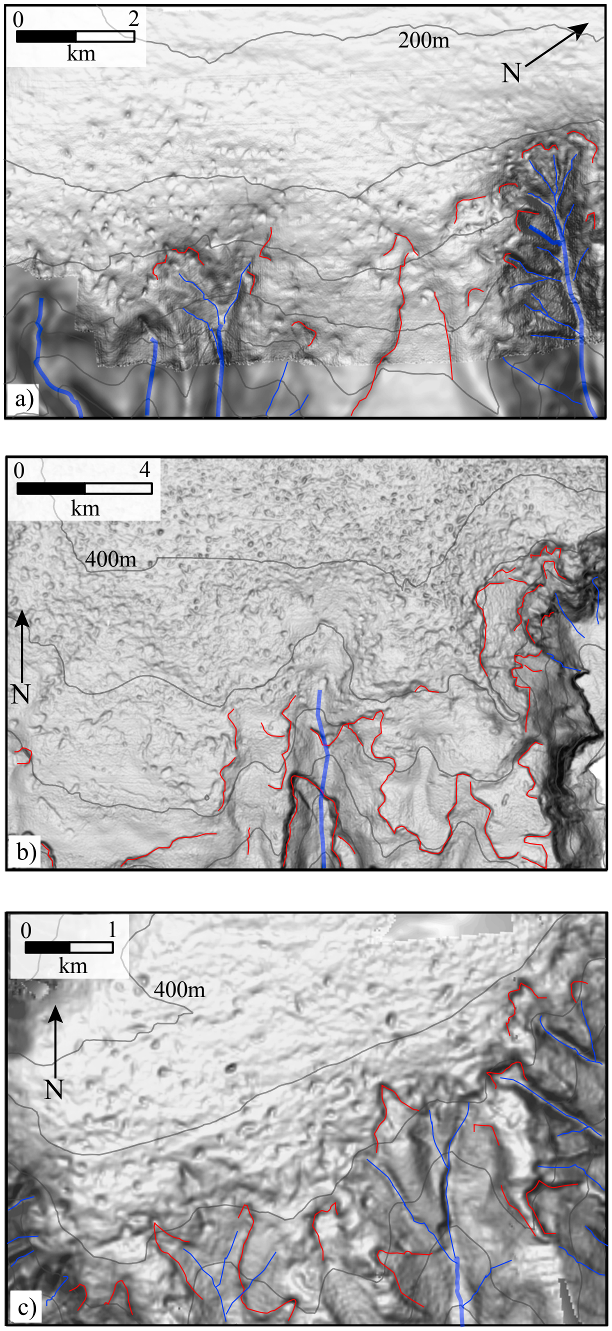

Figure 2. Enlarged shaded relief maps illustrating characteristic pockmark morphology and spatial distribution from select regions (see Figure 1). Pockmarks blanket the shelf edge and upper slope down to water depths of ~700 m, where they either disappear or merge with features associated with mass wasting, such as landslide scarps (red lines) and canyon head gullies (blue lines).

migration pathways [*Ligtenberg*, 2005]. User picks of obvious chimneys and nonchimneys were used to supervise neural network training and the meta-attribute calculation for chimney probability. Seismic horizons below the multiple artifacts were excluded from the interpretation.

[9] The contemporary thickness and upslope extent of the gas hydrate stability zone were calculated using local constraints on bottom water temperatures (BWT) in the vicinity of the MCS profiles and assumed sediment thermal gradients. BWT along the slope were extracted from a composite ocean temperature structure compiled using conductivity-temperature-depth (CTD) measurements located within tens of kilometers of the seismic profiles in the World Ocean Database [*Levitus et al.*, 1998]. Gas hydrate stability was determined using CSMHYD [*Sloan*, 1998] assuming Structure I methane hydrate, 3.5% by weight NaCl in seawater, hydrostatic pressure in the shallow sediments, and a 35 mK m^{-1} thermal gradient, which was based on borehole measurements at Site 1073 [*Austin et al.*, 1998]. Base of gas hydrate stability (BGHS) thicknesses along the two MCS transects were calculated by simultaneous solution of the equations for sediment thermal regimes and for the gas hydrate stability curve (see supporting information).

4. Results

[10] We identify more than 5000 pockmarks along the USAM in depths of 110 to 700 mbsl (Figures 1 and 2). In contrast to the elongated megapockmarks observed offshore Virginia [*Hill et al.*, 2004], the newly discovered pockmarks are mostly semicircular with diameters of 50–500 m (majority 100–200 m; Figure 2) and 5–15 m of relief. Where pockmarks can be resolved, their spatial density ranges from 1 to 15 per km^2, with several generations of superposed pockmarks evident in some areas (e.g., Figure 2b). The across-margin distribution of pockmarks appears to be partially dependent on the morphology of the shelf edge. Pockmarks are confined to areas where the steepness of the seabed is less than 3°–4°, while mass wasting morphologies (e.g., slide scarps, gullies, and canyons) characterize steeper slopes (Figure 2). For example, the majority of pockmarks along the abrupt/angular shelf edge in much of the Mid-Atlantic appear to be confined to a 2–4 km wide band, whereas the broad, gentle, and comparatively uncanyonized shelf slope transition along the Hudson Apron and southern New England margins contains pockmarks across a 5–15 km wide swath of the seafloor. As the local seabed gradient approaches 3°, pockmarks become elongated and open downslope (Figure 2). Although the slope along Proflile-04 contains little-to-no evidence for mass wasting or canyonization processes, we do not observe pockmarks beyond ~700 mbsl.

[11] Using the geometry of shelf edge strata and results from previous studies [*McHugh et al.*, 2010; *Mountain et al.*, 2007], each of the four Pleistocene sequence boundaries identified at Site 1073 (Figure 3a) were extended to profiles located to the north of Hudson Canyon (e.g., Profile-04; Figures 3b and supporting information Figure S1). Beneath the shelf edge, each sequence boundary is associated with erosional truncation and/or toplap. Submarine landslides have removed some of the Pleistocene section along the middle slope of Profile-61 and beyond the seaward limit of Profile-61; lower slope strata show evidence for downlap and complete truncation/bypass where relatively steep (>6°) local slopes are controlled by outcropping Eocene rock [*McHugh et al.*, 1993]. In contrast, the Pleistocene section of Profile-04 shows little to no evidence for slope failure or canyonization, and each successive depositional horizon appears to have mantled the preexisting surface, producing conformable strata from the upper slope to the rise.

[12] Within the Pleistocene section beneath the shelf edge/uppermost slope, we observe the following (Figure 3): (1) highly irregular and discontinuous reflectors that grade

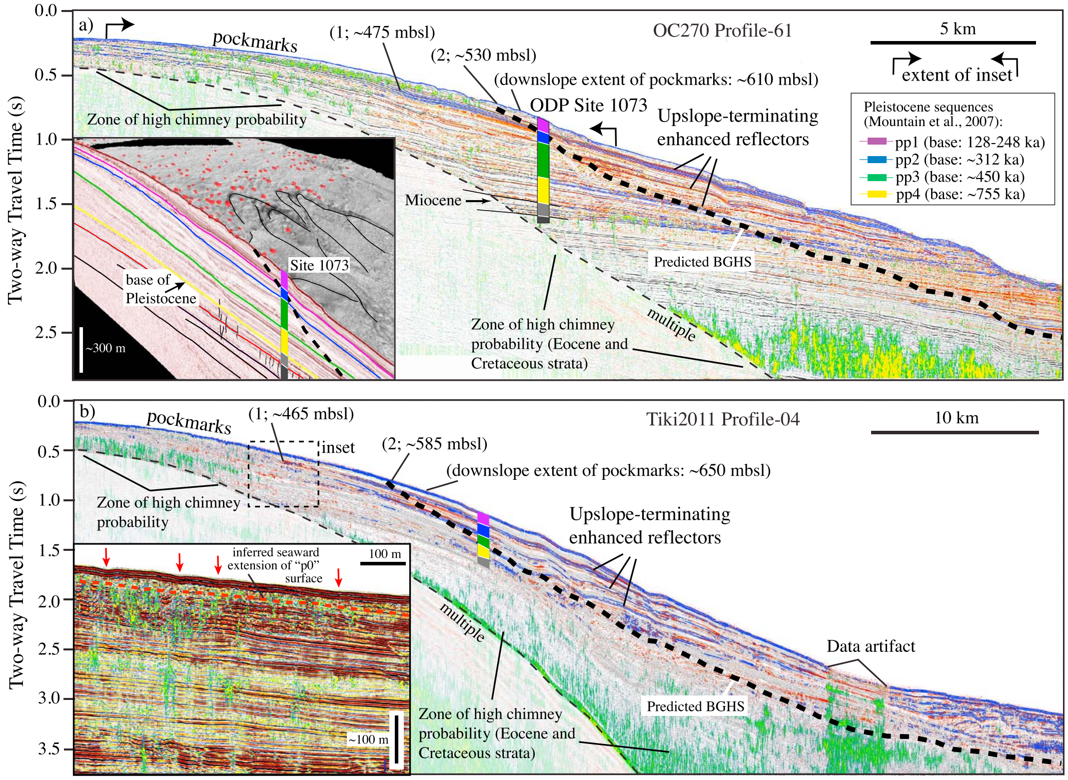

Figure 3. Multichannel seismic reflection profiles along (a) the Hudson Apron (OC270 Profile-61) and (b) southern New England (Tiki2011 Profile-04) sections of the margin (see Figure 1). The chimney probability meta-attribute (green-yellow grades from 50% to 100% probability for fluid pathways), average energy attribute (navy blue = high-energy horizons), and instantaneous frequency (orange-red grades from 160 to 200 Hz) are superposed on standard amplitude traces. Enhanced reflectors (high energy, high frequency) are concentrated above the base of the gas hydrate stability zone (BGHS) and are inferred to represent hydrate-bearing sediments. Hydrate-bearing strata out of equilibrium with present bottom water conditions are bounded by labels "1," the maximum upslope extent of hydrate-bearing sediment, and "2," the top of the gas hydrate stability zone. Inset a: Three-dimensional perspective of pockmarks (red dots), landslide scarps (black lines), and Pleistocene strata (colored lines) [*Austin et al.*, 1998; *Mountain et al.*, 2007]. Inset b: Enlarged section showing chimney probability superposed on standard amplitude traces to highlight evidence for substrate fluidization beneath pockmarks (red arrows).

into concordant and acoustically laminated layers farther downslope (>400 mbsl); (2) discontinuous bright spots of reverse polarity located beneath pockmarks along the uppermost slope; (3) high probability for fluid chimneys beneath pockmarks (Figure 3b inset), but scant evidence for chimneys, within Pleistocene strata of the middle and lower slopes; and (4) gradual, upslope termination of enhanced (positive polarity) reflectors that completely disappear at 400–600 mbsl. We also observe high probability for chimneys within Eocene and Cretaceous strata that are buried along the lower slope (Figure 3).

[13] The high-energy/high-frequency reflectors are largely concentrated within strata immediately up- and down-section of the middle and lower slope equivalents of Pleistocene sequence boundaries (Figure 3). Down section, the enhanced reflectors extend a shorter distance upslope, particularly in Profile-04. The upslope terminations of some of the high-energy reflectors roughly coincide with the calculated BGHS in the upper slope sediments. The calculated updip extent of the gas hydrate stability zone (GHSZ; 530 m on Profile-61 and 580 m on Profile-04) using local BWT constraints also coincides with the seaward transition to lower pockmark density on the upper slope.

5. Discussion

[14] Previous studies noted peculiar stratigraphy along the contemporary and now buried paleo-shelf edges of the Hudson Apron, with each Pleistocene sequence having chaotic internal reflectors that grade into stratified, draping units farther downslope [*Mountain et al.*, 2007]. The spatial coincidence between chaotic and discontinuous strata, high chimney probability, inverse polarity bright spots, and seabed pockmarks suggests that overpressures within Pleistocene sediments are preferentially accommodated by vertical fluid and gas expulsion. Although detailed age constraints are lacking, pockmarks appear to post date an offlap surface linked to the LGM ("p(0)" in *McHugh et al.* [2010]; Figure 3b inset).

[15] Along the Hudson Apron, *Dugan and Flemings* [2002] modeled substrate pore fluid overpressures that resulted from rapid sediment loading along the shelf edge and upper slope during the Late Pleistocene. Fluid flow simulations were based on two substrate architectures: The aquifer model included a permeable Miocene aquifer beneath a low-permeability Pleistocene wedge, while the nonaquifer model did not ascribe higher permeability to the Miocene strata. Our analysis reveals the following: (a) pockmarks, chimneys, disrupted strata, and

headwall landslide scarps (Figure 3a inset) along the shelf edge and upper slope where the aquifer model predicts very low Darcy velocities but also where the nonaquifer model predicts maximum overpressures and (b) acoustically laminated and concordant Pleistocene strata where the aquifer model predicts subhorizontal, seaward flow across Pleistocene stratigraphic boundaries. Furthermore, we observe faults, fractures, and chimneys that pass through or occasionally originate in the inferred Miocene aquifer, suggesting that seaward fluid migration (i.e., aquifer model) in this layer is unlikely. Based on our analysis, the spatial distribution of fluid expulsion features along the margin is most consistent with rapid sediment loading, generation of overpressures, and mostly vertical migration of fluids and gas along the shelf edge and uppermost slope, in accordance with the nonaquifer model of *Dugan and Flemings* [2002]. Despite the general agreement between our observations and the nonaquifer model, a quandary remains in explaining recent and/or ongoing fluid expulsion near some of the upper slope pockmarks [*Skarke et al*., 2013]: The model predicts minimal contemporary fluid expulsion unless recent sources of fluid/gas overpressure can be identified [*Dugan and Flemings*, 2002; *Hustoft et al*., 2009]. In situ generation of gas from microbial processes and dissociation of gas hydrates are both possible sources of recent and/or ongoing gas accumulation in the substrate, leading to expulsion from upper slope sediments of the USAM [*Hill et al*., 2004]. The disappearance of pockmarks downslope is explained by the absence of free gas once the GHSZ is encountered.

[16] Several lines of evidence imply that previously undetected gas hydrates may occur on the upper continental slope on the Hudson Apron/southern New England portion of the USAM. While no reverse polarity bottom-simulating reflector (BSR) is detected at the BGHS along the focus transects, hydrate-bearing sediments (HBS) are known to occur without an underlying BSR in many locations [e.g., *Paull et al*., 1996]. Even in the absence of a BSR, the pattern of enhanced reflectors (Figure 3) terminating upslope roughly matches the morphology of the predicted BGHS. Gas hydrate saturations must reach ~40% of pore space to have an appreciable effect on *P* wave velocities [e.g., *Yun et al*., 2005], but our short-aperture (450-m-long streamer) MCS data yield weak constraints on velocity, and the uppermost 90 m of ODP Site 1073 were not logged [*Austin et al*., 1998]. Even relatively low gas hydrate saturations can increase scattering [*Gei and Carcione*, 2003], an effect that can be captured in the instantaneous frequency attribute. The average energy attribute can enhance small impedance contrasts caused by the changes in elastic moduli associated with the presence of low-saturation gas hydrates [e.g., *Yun et al*., 2005]. In our study area, the enhanced reflectors appear to occur along coarser-grained, more permeable layers that were emplaced during glacial-interglacial transitions [*McHugh and Olson*, 2002]. The high-amplitude/high-frequency character of these coarse-grained reflectors becomes more prominent with distance from the shelf edge (Figure 3), contrary to slope depositional models that predict seaward fining of slope deposits (i.e., lower acoustic impedance) [*Pirmez et al*., 1998]. This implies that some characteristic other than lithology, such as the preferential occurrence of gas hydrate in the coarser-grained, more permeable layers [e.g., *Clennell et al*., 1999], is controlling the reflectivity of these strata. In fact, one of the enhanced reflectors located 70–80 mbsf on Profile-61 was penetrated at ODP Site 1073 [*Austin et al*., 1998]. No gas hydrate was recovered during conventional coring, but this is not surprising if gas hydrate saturations were low. The measured methane concentrations were elevated in this interval, and pore waters were slightly fresher, which would be expected if gas hydrate had been present in situ and had dissociated during core recovery [e.g., *Hesse and Harrison*, 1981]. Site 1073 also has a 6 m thick sulfate reduction zone [*Austin et al*., 1998], consistent with moderate flux of dissolved methane. Within the GHSZ, the attribute analysis reveals no vertical chimneys, which could be consistent with available methane being frozen into gas hydrates. Based on these cumulative observations, we postulate that the high-amplitude/high-frequency enhanced reflectors mapped in Figure 3 may correspond to HBS.

[17] Although the exact origin of gas expulsion remains unknown, the presence of HBS along the upper slope of the USAM may provide a source for recent and/or ongoing gas expulsion due to changes in BWT. The enhanced reflectors and the contemporary upslope extent of the GHSZ overlap with the seaward limit of pockmarks (Figure 3). Enhanced reflectors mapped upslope of the present-day GHSZ may represent HBS that were stranded when intermediate waters impinging on the continental slope were warmed, shifting the GHSZ downslope. Gas hydrate stranded above the BGHS must be out of thermal equilibrium with present-day BWT. If some of the stranded reflectors were at the BGHS prior to warming of impinging ocean waters, gas hydrate stability constraints require the BWT to be 0.6 to 3.8°C cooler than present-day BWT for a conductive thermal gradient of 35°C km^{-1}. One-dimensional thermal modeling shows that warming likely occurred over at most a few decades within the past 20 to 100 years for gas hydrate to persist within these reflectors today. These calculations assume only warming, not the oscillation between cool and warm periods that is more likely over decadal timeframes. The range of warming necessary to explain the possibly stranded upslope HBS in the model brackets the ~1.4°C of warming observed at 500 mbsl the most proximal upper slope CTDs, which were collected in 2002 and 2011. The gradual disappearance of enhanced reflectors between the contemporary updip limit of the GHSZ and water depths as shallow as 475 m (Figure 3) may indicate active disintegration of stranded gas hydrate within the ~475–600 m depth range that marks the seaward limit of pockmarks (Figure 3). Chimneys disrupt the lateral continuity of depositional boundaries beneath the upper slope and provide vertical permeability pathways. Strata within the GHSZ show minimal evidence for chimneys, suggesting that the presence of HBS enhances the integrity of the Pleistocene strata, perhaps inducing updip migration of water and gas toward the upslope limit of the GHSZ. The ability for fluids and gas to migrate updip is expected to diminish at the shelf edge, where strata become horizontal and sediments are generally less cohesive and coarser grained, thus promoting vertical migration and expulsion. Pockmarks located above the shelf edge may have resulted from events that caused transient increases in pore fluid overpressure, such as rapid sedimentation during relative sea level lowstands and peak ground accelerations from earthquakes.

6. Conclusions

[18] The combined effects of compaction-induced pore fluid overpressure and gas hydrate dissociation offer a

plausible explanation for the distribution of pockmarks along the Hudson Apron/southern New England section of the USAM. This interpretation can likely be extrapolated to the pockmarks documented in Figures 1 and 2 and perhaps even to pockmarks on the Canadian Atlantic margin, where evidence for shelf edge fluid expulsion is also widely observed [*Pickrill et al.*, 2001]. Pockmark formation and fluid expulsion at depths between ~475 and 650 mbsl may reflect the combined effects of pore fluid overpressure induced by differential sediment loading [*Dugan and Flemings*, 2002] and gas hydrate dissociation due to transient changes in intermediate water temperatures, although the timing of these processes may be offset by thousands of years. Depending on the geometry of shelf edge strata, it is possible for free gas to migrate farther updip along depositional boundaries and vent at depths significantly shallower than the top of the GHSZ [*Hill et al.*, 2004; *Weibull et al.*, 2010]. Lastly, mapping upper slope gas hydrates has long been a challenge. Advanced attribute analyses applied to high-resolution MCS data may provide better constraints on the fluid plumbing of continental margins and also the distribution of climate-sensitive upper slope gas hydrates on a global basis.

[19] **Acknowledgments.** We thank the NOAA Office of Ocean Exploration for providing bathymetric data and dGB Earth Sciences for the use of OpendTect software package and plug-ins. Laura Brothers provided a very helpful review. We also thank Greg Mountain, Stormy Harrington, Mike Barth, Tom O'Brien, Emile Bergeron, and Eric Moore. The U.S. Geological Survey and the U.S. Nuclear Regulatory Commission funded this research. Any use of trade, firm, or product names is for descriptive purposes only and does not imply endorsement by the U.S. Government.

[20] The Editor thanks Martin Hovland and an anonymous reviewer for their assistance in evaluating this paper.

References

Andrews, B. D., J. D. Chaytor, U. S. ten Brink, D. S. Brothers, and J. V. Gardner (2013), Bathymetric terrain model of the Atlantic Margin for marine geological investigations, *U.S. Geological Survey Open-File Report no. 2012-1266*.

Austin, J. A., et al. (1998), Site 1073, *Proc. Ocean Drill. Program Initial Rep.*, *174A*, 153–191.

Berndt, C. (2005), Focused fluid flow in passive continental margins, *Philos. Trans. R. Soc. A*, *363*(1837), 2855–2871.

Brothers, D. S., U. S. ten Brink, B. D. Andrews, and J. D. Chaytor (2013), Geomorphic characterization of the U.S. Atlantic continental margin, *Mar. Geol.*, *338*, 46–63.

Clennell, M. B., M. Hovland, J. S. Booth, P. Henry, and W. J. Winters (1999), Formation of natural gas hydrates in marine sediments: 1. Conceptual model of gas hydrate growth conditioned by host sediment properties, *J. Geophys. Res.*, *104*(B10), 22,985–23,003.

Dugan, B., and P. B. Flemings (2002), Fluid flow and stability of the US continental slope offshore New Jersey from the Pleistocene to the present, *Geofluids*, *2*(2), 137–146.

Gei, D., and J. M. Carcione (2003), Acoustic properties of sediments saturated with gas hydrate, free gas and water, *Geophys. Prospect.*, *51*, 141–157.

Hesse, R., and W. E. Harrison (1981), Gas hydrates (clathrates) causing pore-water freshening and oxygen isotope fractionation in deep-water sedimentary sections of terrigenous continental margins, *Earth Planet. Sci. Lett.*, *55*(3), 453–462.

Hill, J. C., N. W. Driscoll, J. K. Weissel, and J. A. Goff (2004), Large-scale elongated gas blowouts along the U.S. Atlantic margin, *J. Geophys. Res.*, *109*, B09101, doi:10.1029/2004JB002969.

Hustoft, S., B. Dugan, and J. Mienert (2009), Effects of rapid sedimentation on developing the Nyegga pockmark field: Constraints from hydrological modeling and 3-D seismic data, offshore mid-Norway, *Geochem. Geophys. Geosyst.*, *10*, Q06012, doi:10.1029/2009GC002409.

Judd, A. G., and M. Hovland (2007), *Seabed Fluid Flow: The Impact of Geology, Biology and the Marine Environment*, xv, 475 pp., Cambridge Univ. Press, Cambridge, U.K. and New York.

Levitus, S., T. Boyer, M. Conkright, T. O'Brien, J. Antonov, and C. Stephens (1998), World Ocean Database, National Oceanographic Data Center, NOAA/NESIDS, 18.

Ligtenberg, J. H. (2005), Detection of fluid migration pathways in seismic data: Implications for fault seal analysis, *Basin Res.*, *17*(1), 141–153.

McHugh, C. M. G., and H. C. Olson (2002), Pleistocene chronology of continental margin sedimentation: New insights into traditional models, New Jersey, *Mar. Geol.*, *186*(3-4), 389–411.

McHugh, C. M., W. B. F. Ryan, and B. C. Schreiber (1993), The role of diagenesis in exfoliation of submarine canyons, *AAPG Bull.*, *77*(2), 145–172.

McHugh, C. M., C. A. Hartin, G. S. Mountain, and H. M. Gould (2010), The role of glacio-eustasy in sequence formation: Mid-Atlantic Continental Margin, USA, *Mar. Geol.*, *277*(1-4), 31–47.

Mountain, G., et al. (2007), The long-term stratigraphic record on continental margins, in *Continental Margin Sedimentation: From Sediment Transport to Sequence Stratigraphy*, Blackwell Publishing, Malden, Mass.

Newman, K. R., et al. (2008), Active methane venting observed at giant pockmarks along the U.S. mid-Atlantic shelf break, *Earth Planet. Sci. Lett.*, *267*(1-2), 341–352.

Paull, C., R. Matsumoto, P. Wallace, and W. Dillon (1996), Gas hydrate sampling on the Blake Ridge and Carolina Rise, *Proc. Ocean Drill. Program Initial Rep.*, *164*, doi:10.2973/odp.proc.sr.164.2000.

Phrampus, B. J., and M. J. Hornbach (2012), Recent changes to the Gulf Stream causing widespread gas hydrate destabilization, *Nature*, *490*(7421), 527–530.

Pickrill, R., D. J. W. Piper, J. T. Collins, A. Kleiner, and L. Gee (2001), Scotian Slope Mapping Project: The benefits of an integrated regional high-resolution multibeam survey: Offshore Technology Conference paper OTC 12995, doi:10.4043/12995-MS.

Pirmez, C., L. F. Pratson, and M. S. Steckler (1998), Clinoform development by advection-diffusion of suspended sediment: Modeling and comparison to natural systems, *J. Geophys. Res.*, *103*(B10), 24,141–24,157.

Poag, C. W., and W. D. Sevon (1989), A record of Appalachian denudation in postrift Mesozoic and Cenozoic sedimentary deposits of the U.S. Middle Atlantic continental margin, *Geomorphology*, *2*, 119–157.

Skarke, A., C. D. Ruppel, M. Kodis, E. Lobecker, and M. Malik (2013), Geologic significance of newly discovered methane seeps on the Northern US Atlantic Margin, Abstract OS21A-1613 presented at Fall Meeting, EOS Trans. Amer. Geophys. Union.

Sloan, E. D. (1998), *Clathrate Hydrates of Natural Gases*, Marcel Dekker, New York.

Weibull, W., J. Mienert, S. Bünz, and S. Hustoft (2010), Fluid migration directions inferred from gradient of time surfaces of the sub seabed, *Mar. Pet. Geol.*, *27*(9), 1898–1909.

Yun, T., F. Francisca, J. Santamarina, and C. Ruppel (2005), Compressional and shear wave velocities in uncemented sediment containing gas hydrate, *Geophys. Res. Lett.*, *32*, L10609, doi:10.1029/2005GL022607.